A THREE-PHASE POWER FLOW METHOD FOR REAL-TIME DISTRIBUTION SYSTEM ANALYSIS

Carol S. Cheng
Member

Dariush Shirmohammadi
Senior Member

Energy Systems Automation Group
Pacific Gas and Electric Company
San Francisco, CA

Abstract—This paper presents a three-phase power flow solution method for real-time analysis of primary distribution systems. This method is a direct extension of the compensation-based power flow method for weakly meshed distribution systems[1] from single phase to three-phase, with the emphasis on modeling of dispersed generation (PV nodes), unbalanced and distributed loads, and voltage regulators and shunt capacitors with automatic local tap controls. The method proposed here is capable of addressing these modeling challenges while still maintaining a high execution speed required for real-time application in distribution automation systems. The paper also includes test results from the application of a computer program developed based on the proposed method to large primary electric distribution systems.

Keywords: distribution power flow, distribution automation, real-time power flow.

I. INTRODUCTION

It has been realized that many real-time application programs in the area of distribution automation require a robust and efficient power flow solution method. Such a power flow solution method must be able to model the special features of distribution systems in sufficient detail. Some of the more prominent features of electric distribution systems are:

Radial or near radial structure
Multi-phase, unbalanced, grounded or ungrounded operation
Dispersed generation
Multi-phase, multi-mode control distribution equipment
Unbalanced distributed loads
Extremely large number of branches/nodes

Some power flow techniques that could deal with some of these features have already been developed [1-5]. One type of these algorithms is based on the system admittance matrix and an iteration scheme similar to Newton-Raphson power flow[4,5]. The other type is featured by the compensation-based method with breakpoint impedance matrix[1], along with several efforts on efficient formation of the compensation matrix and handling of PV nodes[2,3].

94 SM 603-1 PWRS A paper recommended and approved by the IEEE Power System Engineering Committee of the IEEE Power Engineering Society for presentation at the IEEE/PES 1994 Summer Meeting, San Francisco, CA, July 24 - 28, 1994. Manuscript submitted August 2, 1993; made available for printing May 17, 1994.

By comparing of these methods, it is seen that the method described in [1] is able to take maximum advantage of the unique topological structure of a distribution system, which is radial or weakly meshed, to achieve high speed, robust convergence and low memory requirement. In addition, the V, I formulation used in [1] allows the extension from single-phase to three-phase to be straightforward.

In this paper we propose a three-phase power flow solution method for real-time analysis of primary distribution systems. The focus of this paper is on several modeling issues related to distribution system operation including unbalanced multi-phase operation, dispersed generation (PV nodes), distributed loads, and voltage regulators and shunt capacitors with automatic tap controls. However, in this paper we do not address other important issues related to a real-time application such as data interfaces and requirements and user interfaces. The overall speed, modeling detail and convergence performance of the algorithm proposed here make it suitable for real-time applications in distribution automation systems.

II. BASIC ALGORITHM FOR POWER FLOW ANALYSIS OF WEAKLY MESHED PRIMARY DISTRIBUTION SYSTEMS

The primary feeders of the distribution system consist of mostly three-phase overhead or underground line sections (branches), and occasionally double-phase or single-phase line sections near the end of the feeder laterals. In the three-phase power flow algorithm, we number each node or line section in the network by a single index, regardless of the number of phases of this node or line section. The series impedance of a line section, l, is represented by a 3×3 matrix:

$$Z_l = \begin{bmatrix} z_{aa,l} & z_{ab,l} & z_{ac,l} \\ z_{ab,l} & z_{bb,l} & z_{bc,l} \\ z_{ac,l} & z_{bc,l} & z_{cc,l} \end{bmatrix} \quad (1)$$

If any phase of the line section does not exist, the corresponding row and column in this matrix contain all zero entries. Figure 1 shows line section l between nodes i and j with shunt admittances and loads attached to each node.

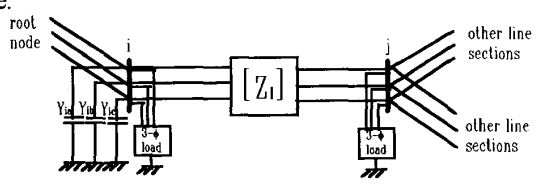

Fig. 1. A three-phase line section

To apply the single-phase power flow algorithm described in [1] to three-phase we first convert the primary distribution network to a radial system by breaking all the loops. Line sections in the radial network are ordered by layers away from the root node (substation bus) as shown in [1], a diagram from [1] is reprinted below.

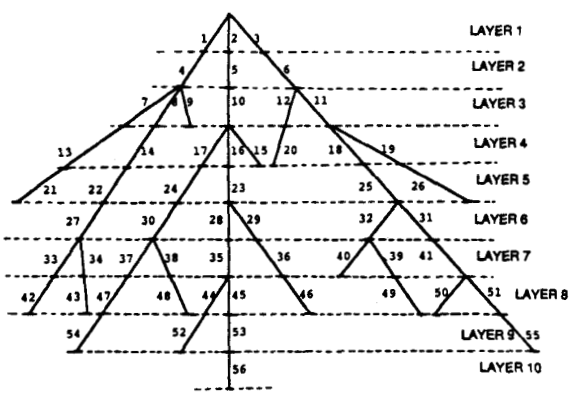

Branch numbering scheme for radial distribution network from Fig. 2 of reference [1]

Let the root node be the slack node with known voltage magnitude and angle, and let the initial voltage for all other nodes be equal to the root node voltage. The iterative algorithm for solving the radial system consists of three steps. At iteration k:

1. Nodal current calculation

$$\begin{bmatrix} I_{ia} \\ I_{ib} \\ I_{ic} \end{bmatrix}^{(k)} = \begin{bmatrix} \left(S_{ia}/V_{ia}^{(k-1)}\right)^* \\ \left(S_{ib}/V_{ib}^{(k-1)}\right)^* \\ \left(S_{ic}/V_{ic}^{(k-1)}\right)^* \end{bmatrix} - \begin{bmatrix} Y_{ia}^* & & \\ & Y_{ib}^* & \\ & & Y_{ic}^* \end{bmatrix} \begin{bmatrix} V_{ia} \\ V_{ib} \\ V_{ic} \end{bmatrix}^{(k-1)} \quad (2)$$

where

I_{ia}, I_{ib}, I_{ic} are current injections at node i corresponding to constant power load and shunt elements

S_{ia}, S_{ib}, S_{ic} are scheduled (known) power injections at node i

V_{ia}, V_{ib}, V_{ic} are voltages at node i

Y_{ia}, Y_{ib}, Y_{ic} are admittances of all shunt elements at node i

Later in the paper we will show how distributed loads along line sections can be converted to lumped loads at system nodes. We will also describe the special case where loads are fed via ungrounded three wire systems.

2. Backward sweep to sum up line section current: starting from the line section in the last layer and moving towards the root node, the current in line section l is:

$$\begin{bmatrix} J_{la} \\ J_{lb} \\ J_{lc} \end{bmatrix}^{(k)} = -\begin{bmatrix} I_{ja} \\ I_{jb} \\ I_{jc} \end{bmatrix}^{(k)} + \sum_{m \in M} \begin{bmatrix} J_{ma} \\ J_{mb} \\ J_{mc} \end{bmatrix}^{(k)} \quad (3)$$

where J_{la}, J_{lb} *and* J_{lc} are the current flows on line section l and M is the set of line sections connected to node j. Note that the negative sign in (3) is to keep consistent with current injections as calculated in (2).

3. Forward sweep to update nodal voltage: starting from the first layer and moving towards the last layer, the voltage at node j is:

$$\begin{bmatrix} V_{ja} \\ V_{jb} \\ V_{jc} \end{bmatrix}^{(k)} = \begin{bmatrix} V_{ia} \\ V_{ib} \\ V_{ic} \end{bmatrix}^{(k)} - \begin{bmatrix} z_{aa,l} & z_{ab,l} & z_{ac,l} \\ z_{ab,l} & z_{bb,l} & z_{bc,l} \\ z_{ac,l} & z_{bc,l} & z_{cc,l} \end{bmatrix} \begin{bmatrix} J_{la} \\ J_{lb} \\ J_{lc} \end{bmatrix}^{(k)} \quad (4)$$

After these three steps are executed in one iteration, the power mismatches at each node for all phases are calculated:

$$\begin{aligned} \Delta S_{ia}^{(k)} &= V_{ia}^{(k)} (I_{ia}^{(k)})^* - Y_{ia}^* |V_{ia}|^2 - S_{ia} \\ \Delta S_{ib}^{(k)} &= V_{ib}^{(k)} (I_{ib}^{(k)})^* - Y_{ib}^* |V_{ib}|^2 - S_{ib} \\ \Delta S_{ic}^{(k)} &= V_{ic}^{(k)} (I_{ic}^{(k)})^* - Y_{ic}^* |V_{ic}|^2 - S_{ic} \end{aligned} \quad (5)$$

If the real or imaginary part (real or reactive power) of any of these power mismatches is greater than a convergence criterion, steps 1, 2 and 3 are repeated until convergence is achieved.

Equations (2)-(5) provide the solution for a three-phase radial network. In a meshed system, it is necessary to simulate loops by injecting currents at both ends of all breakpoints. Currents at breakpoints are calculated using the compensation technique and a breakpoint impedance matrix. This procedure is based on the same principle as described in [1]. Figure 2 shows a three-phase breakpoint, j. For this breakpoint, currents must be injected to all three phases with opposite polarity at the two end nodes, $j1$ and $j2$. These currents are determined in an iteration loop outside the radial power flow solution. At iteration μ,

$$\begin{bmatrix} I_{j1a}^{(\mu)} \\ I_{j1b}^{(\mu)} \\ I_{j1c}^{(\mu)} \end{bmatrix} = -\begin{bmatrix} \hat{J}_{ja}^{(\mu)} \\ \hat{J}_{jb}^{(\mu)} \\ \hat{J}_{jc}^{(\mu)} \end{bmatrix}, \quad \text{and} \quad \begin{bmatrix} I_{j2a}^{(\mu)} \\ I_{j2b}^{(\mu)} \\ I_{j2c}^{(\mu)} \end{bmatrix} = \begin{bmatrix} \hat{J}_{ja}^{(\mu)} \\ \hat{J}_{jb}^{(\mu)} \\ \hat{J}_{jc}^{(\mu)} \end{bmatrix} \quad (6)$$

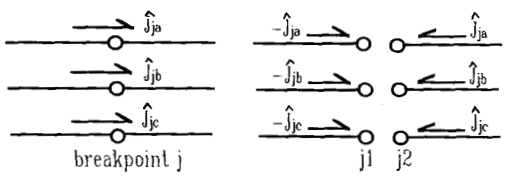

Fig. 2. Three-phase breakpoint representation using nodal current injections

The three-phase currents for all breakpoints are obtained by solving the following complex linear equation:

$$[Z_B][\hat{J}]^{(\mu)} = [\hat{V}]^{(\mu)} \quad (7)$$

where $[\hat{V}]$ is the vector of three-phase voltage mismatches for all breakpoints and $[Z_B]$ is a constant complex matrix, referred to as the breakpoint impedance matrix. The physical meaning and the formation of $[Z_B]$ for single-phase systems have been well explored in [1]-[3]. For three-phase systems, since all the loops are likely to be among three-phase line sections, the break point impedance matrix mainly consists of 3×3 block submatrices. Numerically, the diagonal submatrix Z_{ii} is equal to the sum of the line section impedance matrix in (1) for all the line sections in loop i. The off-diagonal submatrix, Z_{ij}, is nonzero only if loop i and loop j share one or more common line sections. The signs of the off-diagonal submatrices depend on the relative direction of the breakpoint current injections for loops i and j.

In our algorithm, $[Z_B]$ is formed and factorized at the beginning before any iteration is performed. After each radial power flow is converged, the three-phase voltage mismatches at all breakpoints are compared with a threshold. If the mismatch of any breakpoint of any phase is greater than the threshold, (7) is solved and the breakpoint current $[J]$ is updated. This iteration process continues until all the breakpoint voltage mismatches are less than the threshold.

III. COMPENSATION FOR PV NODES

Since dispersed generators are becoming prevalent in distribution systems, modeling them in a distribution power flow algorithm has become an inevitable task. Depending on the contract and control status of a generator, it may be operated in one of the following modes:

1. In "parallel operation" with the feeder, i.e., the generator is located near and designated to supply a large load with fixed real and reactive power output. The net effect is the reduced load at a particular location.
2. To output power at a specified power factor.
3. To output power at a specified terminal voltage.

In power flow context, the generation nodes in the first two cases can be well represented as PQ nodes, which require little special treatment in the power flow algorithm. The generation node in the third case must be modeled as a PV node. Special procedures must be performed to maintain its voltage magnitude as well as to monitor its reactive power capability.

We have developed a compensation method using a PV node sensitivity matrix to eliminate the voltage magnitude mismatch for all PV nodes. The basic idea of this method can be explained as follows. Suppose a power flow as described in Section II has converged, and the voltage magnitude at PV nodes are not equal to the scheduled values. In order to obtain the scheduled voltage magnitude at a PV node, we need to determine the correct amount of reactive power or reactive current injection generated by the unit. Therefore, the problem of compensating PV node voltage magnitude becomes: Find the reactive current injection, I_q, for each PV node so that the voltage magnitude, $|V|$, of this node is equal to the scheduled value. Since the relation between I_q and $|V|$ is nonlinear, I_q can only be determined iteratively. A PV node sensitivity matrix is introduced to approximate the nonlinear relation between $|V|$ and I_q and is used to evaluate I_q iteratively as described below.

3.1 PV Node Sensitivity Matrix

A PV node is modeled in a similar manner as in [5], i.e., the constants for a generator are the three-phase real power output and the magnitude of the positive sequence voltage. The use of positive sequence representation for voltage magnitude regulation makes it possible to properly represent the automatic voltage regulation (AVR) mechanism of a generating unit, where in most cases, the average of voltage magnitude of all three phases is the voltage magnitude that is regulated.

The incremental relation between the magnitude of positive sequence voltage and the magnitude of the positive sequence reactive current injection is expressed as

$$[Z_V][I_q]^{(\gamma)} = [\Delta V]^{(\gamma)} \quad (8)$$

where $[Z_V]$ is a constant real matrix, referred to as the PV node sensitivity matrix. The dimension of $[Z_V]$ is equal to the number of PV nodes. Column j of $[Z_V]$ may be determined by applying $Ij = \{0.,1.\}$ to PV node j with all loads and sources removed, and solving a positive sequence network with one back and forward sweep for the change of voltage magnitudes at all PV nodes.

Equivalently, $[Z_V]$ can be formed by observing the following numerical properties of its entries. The diagonal entry, z_{ii}, in $[Z_V]$ is equal to the modulus of the sum positive sequence impedance of all line sections between PV node i and the root node (substation bus). If two PV nodes, i and j, have completely different path to the root node, then the off-diagonal entry z_{ij} is zero. If i and j share a piece of common path to the root node, then z_{ij} is equal to the modulus of the sum positive sequence impedance of all line sections on this common path. Based on these, $[Z_V]$ can be formed by identifying the path between PV nodes and the root node. When forming $[Z_V]$ for a group of feeders connected to different substations, the impedance paths will be between the PV node on a feeder and the substation bus (root node) to which the feeder is connected.

In our power flow algorithm, $[Z_V]$ is formed for all initial PV nodes and factorized into LU before any power flow iteration is performed. Depending on whether there are PV to PQ node conversions, $[Z_V]$ and its factors may have to be updated, as to be described in section 3.2.

3.2 Iterative Process for Voltage Magnitude Correction

Suppose there are n PV nodes in a system. The reactive current injections at these PV nodes are determined through an iteration loop outside the breakpoint current compensation. Each time after the breakpoint voltage mismatches are reduced below a threshold, the following steps are performed to correct the voltage magnitude at all PV nodes. At iteration γ:

1. Calculate positive sequence voltage magnitude mismatch for all PV nodes

$$\Delta V_i^{(\gamma)} = \left|V_i^s\right| - \left|V_i^{(\gamma)}\right| \qquad i = 1, 2, \ldots, n \tag{9}$$

Where V_i^s is the scheduled voltage magnitude for node i. If any of these mismatches is greater than a threshold, then perform the next step:

2. Solve for PV node reactive current injection using (8). The solution provides a linear approximation of the reactive current injection needed to eliminate the voltage magnitude mismatch in this iteration. If the reactive power generations were unlimited, we would inject I_{iqa}, I_{iqb}, I_{iqc} at 90 degrees leading the corresponding voltage V_{ia}, V_{ib}, V_{ic} at each PV node, i:

$$\begin{aligned} I_{iqa}{}^{(\gamma)} &= \left|I_{iq}\right|^{(\gamma)} e^{j(90^o + \delta_{Via}^{(\gamma)})} \\ I_{iqb}{}^{(\gamma)} &= \left|I_{iq}\right|^{(\gamma)} e^{j(90^o + \delta_{Vib}^{(\gamma)})} \\ I_{iqc}{}^{(\gamma)} &= \left|I_{iq}\right|^{(\gamma)} e^{j(90^o + \delta_{Vic}^{(\gamma)})} \end{aligned} \tag{10}$$

where δ_{Via}, δ_{Vib}, δ_{Vic} are voltage angles of the three phases of the PV node. Since in reality the reactive power capability of a generator is always limited, the reactive power limits must be checked first to determine whether the required current injections are available, as in the next step:

3. Calculate the required reactive power generation Q_{ig} for all PV nodes:

$$Q_{ig}^{(\gamma)} = Q_i^{'(\gamma)} + Q_{id} \qquad i = 1, 2, \ldots, n \tag{11}$$

where Q_i' is the new reactive power injection at node i. It is calculated using the PV node voltage and the new current injection:

$$Q_i^{'(\gamma)} = \mathrm{Im}\left[V_{ia} I_{ia}'^{*}\right]^{(\gamma)} + \mathrm{Im}\left[V_{ib} I_{ib}'^{*}\right]^{(\gamma)} + \mathrm{Im}\left[V_{ic} I_{ic}'^{*}\right]^{(\gamma)} \tag{12}$$

The new current injection at PV node i is a combination of the desired reactive current injection and load current injection:

$$\begin{aligned} I_{ia}'^{(\gamma)} &= I_{iqa}^{(\gamma)} + I_{ia}^{(\gamma)} \\ I_{ib}'^{(\gamma)} &= I_{iqb}^{(\gamma)} + I_{ib}^{(\gamma)} \\ I_{ic}'^{(\gamma)} &= I_{iqc}^{(\gamma)} + I_{ic}^{(\gamma)} \end{aligned}$$

Q_{id} in (11) is the scheduled reactive load at PV node i.

4. Q_{ig} then is compared with the reactive power generation limits. If Q_{ig} is within the limits, i.e.,

$$Q_{ig}^{\min} < Q_{ig}{}^{(\gamma)} < Q_{ig}^{\max}$$

then the corresponding reactive current, I_{iqa}, I_{iqb}, I_{iqc} are injected to PV node i according to (11). In subsequent iterations, these currents will be combined with other nodal current injections. Otherwise, if Q_{ig} violates any reactive power generation limit, it will be set to that limit, divided by three for three phases and combined with the reactive load of each phase at this node. Subsequently, the row and column in the PV node sensitivity matrix, $[Z_V]$, corresponding to this node are removed and the LU factors of $[Z_V]$ are updated.

The iteration described in steps 1-4 will continue until the voltage magnitude mismatches for all PV nodes as calculated in (8) become less than a threshold.

The flow chart of overall power flow algorithm is shown in Figure 3. It is seen that the algorithm consists of three nested iteration loops for radial power flow, breakpoint voltage compensation and PV node voltage magnitude compensation, respectively. The termination of each iteration loop is controlled by a threshold. Our experience shows that once the breakpoint compensation starts after the initial iterative radial power flow, subsequent radial power flows always converge in one or two iterations under the same threshold for power mismatches. The same pattern has been observed between PV node compensation and the breakpoint compensation.

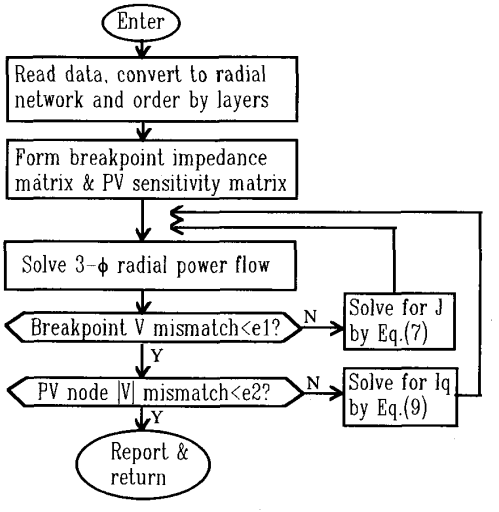

Fig. 3. Flow chart of the power flow algorithm

IV. OTHER MODELING ISSUES FOR DISTRIBUTION SYSTEMS

This section addresses several practical modeling issues involved in the three-phase power flow algorithm.

4.1 Distributed Loads

In a distribution system, a primary feeder supplies loads through distribution transformers tapped at various locations along line sections. If every load point were to be modeled as a node, the number of nodes in a system would become prohibitively large. In our power flow algorithm, we model these distributed loads by approximating their effect on nodal voltage magnitude via equivalent lumped loads.

Consider any phase of a line section of length L shown in Figure 4(a). Suppose the load is uniformly distributed along the line section with the total value of $P+jQ$. We want to lump a portion of the total load at one end node and the rest at the other, as shown in Figure 4(b), such that the voltage magnitude drop at node 2 is the same as that caused by the distributed load along the line. In our derivation, we assume that the voltage angles at both nodes 1 and 2 are small and negligible. This assumption is based on the examination of many numerical results which have consistently shown that the angle deviation for an entire feeder is usually no larger than a few degrees. We also assume that there is a linear drop of the voltage magnitude along the line section, i.e.,

$$v(x) = \frac{V_2 - V_1}{L} x + V_1 \tag{13}$$

where x is any point on the line section measured from node 1, as shown in Figure 4(c). The current flowing in the line section is a function of x:

$$i(x) = \int_x^L \left(\frac{P + jQ}{Lv(y)} \right)^* dy \tag{14}$$

The voltage drop across the line section is

$$\Delta V = \int_0^L i(y)(\eta + jx_l)dy \tag{15}$$

where r_l+jx_l is the impedance per unit length of the line (ohms/meter). This voltage drop should be equal to that caused by the equivalent lumped load at node 2, $\eta(P + jQ)$:

$$\int_0^L i(y)(r_l + jx_l)dy = \eta \left(\frac{P + jQ}{V_2} \right)^* (R_l + jX_l) \tag{16}$$

where η denotes the portion of the line section total load $P+jQ$ that is lumped at the end node, $0.0 < \eta < 1.0$, and $R_l + jX_l$ is the line section impedance. Substitute (14) into (16), integrate the left-hand-side and solve for η, we have

$$\eta = \frac{V_2}{(V_2 - V_1)^2} \left[V_1 In \frac{V_1}{V_2} + (V_2 - V_1) \right] \tag{17}$$

Figure 5 shows the variation of η with different values of V_1 and V_2. It is seen that η varies around 0.5 in a fairly narrow range as the voltages at the two end nodes assume different values. Since the voltage drop across a single line section is usually small ($V_1 \cong V_2$), it is reasonable to choose η to be 0.5. Based on this observation, in our power flow algorithm, the total distributed load on each phase of a line section is lumped half-half at the line section's two end nodes.

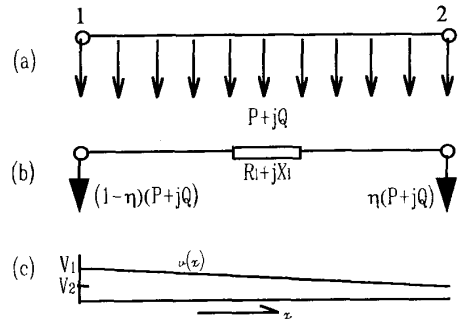

Fig. 4. Equivalencing distributed loads to lumped loads

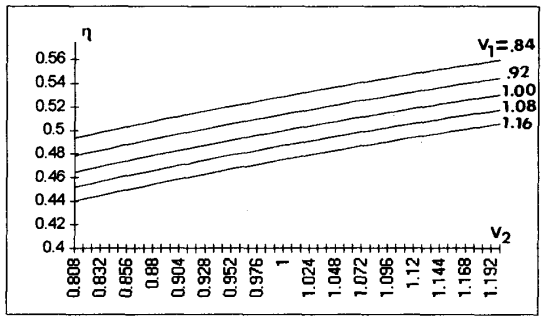

Fig. 5. Variation of η as a function of V

4.2 Load Representation for Three Wire Ungrounded Systems

In practice, some distribution feeders are constructed as three wire systems without ground wire (a common practice in Pacific Gas and Electric Company). Loads of each phase are supplied through distribution transformer connected between two phases of the primary feeder, as illustrated in Figure 6.

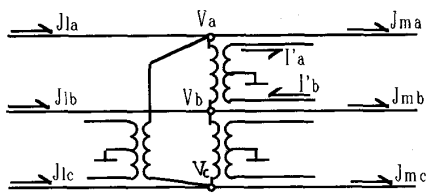

Fig. 6. Load supplied via three wire system

In this case, the load cannot be decomposed by phases and the following equations should be used in the back sweep to replace equations (2) and (3):

$$\begin{bmatrix} I_{iab} \\ I_{ibc} \\ I_{ica} \end{bmatrix}^{(k)} = \begin{bmatrix} \left(S_{iab}/V_{iab}^{(k-1)}\right)^* \\ \left(S_{ibc}/V_{ibc}^{(k-1)}\right)^* \\ \left(S_{ica}/V_{ica}^{(k-1)}\right)^* \end{bmatrix} - \begin{bmatrix} Y_{iab}^* & & \\ & Y_{ibc}^* & \\ & & Y_{ica}^* \end{bmatrix} \begin{bmatrix} V_{iab} \\ V_{ibc} \\ V_{ica} \end{bmatrix}^{(k-1)} \quad (18)$$

$$\begin{bmatrix} J_{la} \\ J_{lb} \\ J_{lc} \end{bmatrix}^{(k)} = \begin{bmatrix} 1 & 0 & -1 \\ -1 & 1 & 0 \\ 0 & -1 & 1 \end{bmatrix} \begin{bmatrix} I_{jab} \\ I_{jbc} \\ I_{jca} \end{bmatrix}^{(k)} + \sum_{m \in M} \begin{bmatrix} J_{ma} \\ J_{mb} \\ J_{mc} \end{bmatrix}^{(k)} \quad (19)$$

where S_{iab}, S_{ibc} and S_{ica} are the total load located between phases ab, bc and ca, respectively. Other distribution equipment connected to an ungrounded system are also connected between phases and their V-I characteristics can be directly modeled in this solution technique.

4.3 Voltage Regulators

Voltage along primary feeders are often controlled by voltage regulators. These regulators are auto-transformers with individual taps on their windings. Typically, the regulator is used to boost (increase) or buck (decrease) the voltage by a variable amount up to 10 percent. A regulator can be operated in manual mode or automatic mode. In the manual mode, the output voltage can be manually raised or lowered on the regulator's control board. In the automatic mode, the regulator control mechanism adjusts the taps to assure that the voltage being monitored is within certain range.

The proposed three-phase power flow algorithm is capable of modeling Y connected three-phase voltage regulators operating in both modes. The regulator in each phase is represented by a series impedance and an ideal transformer with taps on the secondary. In the manual mode, the tap position is known and so is the turns ratio of the ideal transformer. Thus during the back-forward sweep in the radial power flow solution, the turns ratio will be applied to the line section current calculation and the node voltage calculation wherever the regulator is encountered. In the automatic mode, the tap position is unknown prior to the power flow solution. It will be adjusted within the radial power flow algorithm in order to simulate the regulator's automatic tap-control mechanism.

Specifically, the tap positions of all regulators in automatic mode are first initialized to the neutral position (neither boost nor buck) before power flow iterations. During the forward sweep in a radial power flow solution, the following steps are performed when such a regulator is encountered. At iteration k:

1. Calculate the secondary voltage, V_s, of each phase of the regulator using the given tap values, and check if the voltage is within the lower and upper limits of the regulated voltage setting:

$$\left|V_s^{\min}\right| < \left|V_s^{(k)}\right| < \left|V_s^{\max}\right| \quad (20)$$

or

$$\left|V_s^{\min}\right| < \left|V_s^{(k)} - J_s^{(k)}(R_T + jX_T)\right| < \left|V_s^{\max}\right| \quad (21)$$

where (21) is to simulate the line drop compensation (LDC) scheme. This scheme requires a regulator to maintain voltage at some point remote from itself by means of the dial settings on the regulator's control panel. In (21), R_T, X_T are the resistance and reactance calculated approximately from the LDC's R, X settings, and $J_s^{(k)}$ is the secondary line section current obtained during the back sweep.

2. If $V_s^{(k)}$ is greater than the upper limit, set $V_s^{(k)}$ to the limit, calculate the new tap position and round it up to the nearest lower tap position. If $V_s^{(k)}$ is less than the lower limit, set $V_s^{(k)}$ to the limit, calculate the new tap position and round it up to the nearest upper tap position.

3. Check if the tap position obtained in step 2 exceeds the maximum boost or buck limits. If it does, set the tap at the corresponding limit.

4. Re-calculate $V_s^{(k)}$ using the new tap value and continue the forward sweep.

With these steps, the tap positions of regulators in automatic mode will be determined after each radial power flow solution. This assures that the regulated voltage is within the desired range. Since in primary feeders there are usually only a few voltage regulators with automatic tap-changing mechanism, the addition of the above steps into the forward sweep of the radial power flow algorithm has no noticeable effect on the overall solution speed .

4.4 Shunt Capacitors

Shunt capacitors are often used in primary feeders to improve voltage profile and reduce line losses. Most shunt capacitors are equipped with a local control scheme for switching on-line or off-line according to certain conditions. The most commonly-monitored parameters for capacitor control are time, temperature, voltage, current, KVAR and power factor. In practice capacitor controls use combination of these parameters, such as time control with voltage override or temperature control with voltage override.

The three-phase power flow algorithm is capable of handling each of these controls. The following general procedures are used to simulate the automatic local control scheme of capacitors:

1. For those capacitors with time or temperature control, initialize their on/off statuses based on given time and temperature and keep these statuses fixed during the power flow solution.

2. For those with other controls, initialize their on/off statuses based on given time or temperature, or initialize their statuses to off if time or temperature is not monitored.

3. In the outermost iteration loop, check the monitored quantity against the setting. For example, the monitored quantity is the node voltage at the capacitor bank, and the system has PV nodes. In this case, the outermost iteration loop is the PV node compensation loop. Once the PV node compensation is finished in one iteration, the monitored voltage will be compared to the capacitor setting.

4. Modify the on/off statuses of all capacitors according to the comparison results obtained in step 3 and continue for the next radial power flow solution.

The power flow is considered to have converged if all convergence criteria are satisfied, plus there is no further change in capacitors on/off statuses. The capacitor control logic actually adds one more condition for the termination of the outermost iteration loop (see Figure 3).

V. RESULTS

Based on the proposed solution algorithm, we developed a three-phase distribution power flow program, DISFLO, as one of the real-time applications for distribution automation systems. The program was tested using typical primary distribution feeders in PG&E. The test system presented here consists of two large primary feeders supplied by a 21kv substation. These two feeders are of radial structure with 233 switches at various locations. In our test, these switches were opened and closed to simulate different system topologies and different number of loops. Also since it is expected that in the near future increasing number of dispersed generators will be directly connected to primary distribution feeders, PV nodes were introduced at various locations for testing purposes. Other major features of the system are listed below:

No. of line sections : 1418 (Multi-phase), 3368 (actual)
No. of nodes : 1419 (Multi-phase), 3371 (actual)
No. of capacitors : 20 (with adjustable on/off status)
No. of regulators : 3 (with adjustable taps)

Table 1 shows the solution efficiency as the numbers of loops and PV nodes are varied in the system. The elapsed execution time is measured on a single CPU SUN Sparc10 workstation. This time includes the execution of all steps illustrated in Figure 3 except "read data" in the first box, and "report" in the last step.

It is seen that the proposed solution algorithm is efficient despite the large system size and the complexity of system equipment. As the number of loops and PV nodes is increased, the execution time increases less than linearly. This feature is favorable for large primary distribution systems at present and in the near future, where more and more dispersed generators and controllable devices are expected to be connected to or installed in primary feeders.

Table 1 Execution Time in Seconds on SUN Sparc10

# of loops ⇒ / # of PV nodes ⇓	0	2	5	10	30
0	1.46	1.51	1.52	1.68	2.05
10	1.71	1.90	2.02	2.40	2.41
20	2.17	2.42	2.43	3.51	3.94
40	2.73	3.25	3.47	4.24	6.07

The high execution speed may be attributed to two factors. First, the radial power flow solution algorithm with backward and forward sweeps, successfully used with loop compensation as proposed in [1], is very efficient, particularly for large systems, as shown in Table 2. Note that the solution time increases only linearly with system size. Second, only small and constant matrices need to be formed for the breakpoint voltage compensation and the PV node voltage magnitude compensation. The dimensions of these matrices are equal to the number of loops and the number of PV nodes, respectively, which are substantially smaller than the dimension of impedance or admittance matrices in traditional power flow solution techniques. These matrices need to be formed and factorized only once for each power flow solution, and only the factors of the PV node sensitivity matrix need to be updated for PV/PQ node conversions. These features not only make the execution speed less sensitive to the number of loops and PV nodes, but also keep the requirement of computer memory resources at a minimum.

Table 2 Execution Time for Three-phase Radial Systems

No. of multi-phase nodes (line sections)	Actual No. of nodes (line sections)	Time (seconds)
690	1555	0.69
1419	3371	1.46
2479	5983	2.39

The proposed three-phase power flow algorithm is also very robust. Convergence has been reached for all the cases tested. Monotonous convergence pattern has been observed for the radial power flow (innermost iteration loop) and for breakpoint voltage compensation (second iteration loop). The PV node compensation converges almost monotonically. A typical convergence pattern for PV node compensation for the 1419 node system (with 40 PV nodes and 30 loops) is shown in Table 3. The slight fluctuation of the maximum voltage mismatch is caused by introduction of other reactive power sources via capacitor switching, as well as by PV/PQ node conversions.

Table 3 Typical Convergence Pattern for PV Node Voltage Magnitude Compensation
(1419 nodes, 30 loops, 40 PV nodes)

Iteration No.	max(|ΔV|) / V_{rated} (V_{rated}= 12kv)
$\gamma = 1$	0.03443
$\gamma = 2$	0.04154
$\gamma = 3$	0.04095
$\gamma = 4$	0.03878
$\gamma = 5$	0.006187
$\gamma = 6$	0.002135
$\gamma = 7$	0.0006860
$\gamma = 8$	0.0003218
$\gamma = 9$	0.00008039

In summary, the speed and robustness of this solution algorithm makes it suitable for real-time application in distribution automation systems.

VI. CONCLUSIONS

This paper presents a unique three-phase power flow solution method for large distribution systems. The kernel of this method is an efficient three-phase radial power flow with breakpoint voltage compensation, extended from its single-phase version proposed earlier in [1]. The idea of compensation is also employed successfully to eliminate the voltage magnitude mismatches at PV nodes, thus making this method capable of handling dispersed generation in primary distribution systems. Other issues involved in distribution system operation, such as multi-phase operation with unbalanced and distributed loads, regulators and capacitors with automatic tap controls, can also be addressed within the algorithm. Test results show that the method is efficient and robust, and hence suitable for analyzing the real-time operation of large primary distribution systems. We have developed the computer program DISFLO based on this algorithm for use in PG&E's distribution automation systems.

VII. ACKNOWLEDGMENT

The authors would like to thank Mssrs. Brian Agnew, Robert Hartwell, Tom Hillesland, Bill Lemon, Paul Mauldin, Farajollah Soudi and Jimmie Yee of PG&E for their useful comments in the development of this algorithm. PG&E R&D department funded the development of the DISFLO program.

REFERENCES

[1] D. Shirmohammadi, H. W. Hong, A. Semlyen and G. X. Luo, "A Compensation-based Power Flow Method for Weakly Meshed Distribution and Transmission Networks", IEEE Trans. on Power Systems, Vol. 3, No. 2, May 1988, pp.753-762.

[2] G. X. Luo and A. Semlyen, "Efficient Load Flow for Large Weakly Meshed Networks", IEEE Trans. on Power Systems, Vol. 5, No. 4, November 1990, pp.1309-1316.

[3] D. Rajicic, R. Ackovski and R. Taleski, "Voltage Correction Power Flow", Paper 93 WM 060-4 PWRD, presented at the IEEE/PES 1993 Winter Meeting, Columbus, OH, Jan. 31 - Feb. 5, 1993.

[4] T.-H. Chen, M.-S. Chen, K.-J. Hwang, P. Kotas and E. A. Chebi, "Distribution System Power Flow Analysis - a Rigid Approach", IEEE Trans. on Power Delivery, Vol. 6, No. 3, July 1991, pp.1146-1152.

[5] W. Xu, J. R. Marti and H. W. Dommel, "A Multiphase Harmonic Load Flow Solution Technique", IEEE Trans. on Power Systems, Vol. 6, No. 2, Feb 1991, pp. 174-182.

Carol S. Cheng (M'92) was born in Beijing, China. She received her B.S. in Electrical Engineering from Northern Jiaotong University in Beijing in 1982, M.S. in Mechanical Engineering from the University of Cincinnati in 1986, and Ph.D. in Electrical Engineering from Georgia Institute of Technology in 1991. From 1982 to 1985, she worked for Northern Jiaotong University as a Teaching Assistant. Since 1992 she has joined PG&E as a Consulting Engineer. Her current research interests include steady state power system analysis methodologies and their application in distribution automation systems.

Dariush Shirmohammadi (SM'89) received his B.Sc. in Electrical Engineering from Sharif University of Technology in 1975 and M.A.Sc. and Ph.D. in Electrical Engineering from the University of Toronto in 1978 and 1982 respectively. Between 1977 and 1979, he worked in Hydro Quebec Institute of Research (IREQ) on the subject of external insulation. Between 1982 and 1985, Dariush worked in Ontario Hydro on the development and application the EMTP. Dariush worked with the Systems Engineering Group of the Pacific Gas and Electric Company (PG&E) between 1985 and 1991 where he developed advanced methodologies and computer models for the analysis, optimization and costing of transmission and distribution networks. Presently, Dariush is with the Energy Systems Automation Group of PG&E where he is responsible for the development and implementation of automation technologies in electric distribution system operation. Dariush is a registered Professional Engineer in the Province of Ontario, Canada.

Discussion

Hormoz Kazemzadeh and Fan Zhang (ABB Automated Distribution Division, 1021 Main Campus Drive, Raleigh, NC 27606-5202) Congratulations to the authors for providing such a practical and well-organized paper. It has been known for some time that some special power flow methods are computationally more attractive than Newton-Raphson type methods in solving the power flow of distribution systems without considering PV nodes. This paper extends one of these methods by taking the PV nodes into account. Authors opinions on the following issues would be appreciated:

a) What are the assumptions (e.g. voltage angles among all buses are small, high x/r ratio etc.) you make to derive the equation (8) from its corresponding complex equation, such that the real power computed by the equations similar to equations (11) and (12) is close to the desired real power ? Did you encounter any divergent cases if the test system hardly satisfies the assumptions ?

b) How sensitive is the computation performance versus the initial reactive power injection for PV nodes? What is your suggested initial value? Is it taken as zero, based on an assumed power factor, or other ?

c) How is the computation performance changed (better or worse) if the iteration loops for breakpoint voltage compensation and PV node voltage magnitude compensation are combined in one iteration loop, or if the order of these two iteration loops is reversed?

d) Distribution systems are usually unbalanced due to unbalanced loading of the different phases. The authors may consider using a 4x4 line impedance matrix (equation 1) to properly represent neutral current due to unbalance.

e) The method of backward and forward sweep (otherwise known as the Ladder Technique) is based totally on node voltages. It seems more logical to use a voltage mismatch criteria, rather than a power mismatch criteria (step 3), at the root node.

f) However infrequent, sources are sometimes tied together in distribution systems for short periods of time. A real-time power flow must be able to model parallel sources. Authors experience in modeling parallel sources using your own method would be appreciated.

Manuscript received August 9, 1994.

Carol S. Cheng and Dariush Shirmohammadi: The authors would like to thank the discussors for their interests in the paper and their thoughtful questions. Our opinions on each item are as follows:

a) We derived Equation (8) based on a sensitivity study of PV node voltage magnitude with respect to PV node reactive current injection at no load condition. No special assumptions were made for this purpose. We neglected all shunt elements. During the PV node compensation, this equation is solved in each iteration to provide the correct magnitude of the positive-sequence reactive current injection. The angle of the reactive current injection for each phase is determined according to the voltage angle in each iteration, i.e., the reactive current for each phase is always injected at 90° leading its node voltage of the same phase. In this way, the injected current contributes only to the reactive power component at this node. The real power output of each unit remains unchanged throughout the power flow solution.

Based on our test results, convergence characteristics of the proposed algorithm is insensitive to loading conditions and network parameters. The test system we described in the paper has an x/r ratio ranging from 0.1968 to 5.0. Voltage angles up to 15° has been observed (under loading conditions particularly set for testing purpose and multiple substations). Convergence has been reached with approximately the same number of iterations for all the cases we tested.

b) A good initial guess for the reactive power injections at PV nodes will result in smaller initial voltage magnitude mismatches and thus will speed up the convergence of the algorithm. It will also lead to more accurate predictions of PV/PQ conversions. In our test, however, we used zero initial reactive power for all generating units, due to the simulated nature of the entire generation data. It is definitely useful if some heuristics can be derived to predict the initial reactive power for all generating units, since real-time measurements for co-generating units are less likely to become available.

c) We tested an algorithm in which the PV node voltage magnitude is compensated first and the breakpoint voltage mismatch is reduced later on a 35 node system with 4 PV node placed at various locations, and under different loading conditions. The algorithm tends to diverge. We have not tried to combine the breakpoint impedance matrix and the PV node sensitivity matrix in order to compensate both in one iteration loop, because the former is a complex matrix based on three-phase parameters and the later is a real matrix based on positive-sequence parameters.

The reason that we use the proposed compensation sequence, i.e., eliminating the voltage mismatch at breakpoints followed by eliminating the voltage magnitude mismatch at PV nodes, is based on the following observations: the reactive power injection at each PV node and its voltage magnitude adjustment is mainly a local effect. The relation between PV node voltage magnitude and reactive power injection is more nonlinear than the relation between breakpoint voltage and breakpoint current injection. Therefore the calculation of PV node reactive current injection (i.e., solution of equation (8)) should be done using the best guess of the system state in that iteration, where everything is satisfied for a solution except the PV node voltage magnitude. In this way, the nonlinearities involved in this compensation are confined to such a level that a linear equation (8) serves as a valid approximation of the actual gradient leading to convergence.

d) We fully agree with the discussors on using a 4×4 line impedance matrix. We used the 3×3 line impedance matrix since most feeders in our system are 3-wire feeders, and neutral impedance are not readily available. The proposed algorithm can be readily extended to accommodate the 4×4 line impedance matrix. Preferably, standard methods of reducing 4×4 impedance matrices to 3×3 matrices can be used to account for ground wire effect.

e) We use the power mismatch criteria at every node as condition of convergence. This is considered the only accepted criterion to guarantee true convergence for power flow algorithms.

f) The proposed algorithm is able to model multiple parallel sources, typically multiple substations. Each substation is modeled as a slack node with known voltage magnitude and angle.

Manuscript received September 9, 1994.